

CHAPTER
3.2

CORRELATING QUANTITATIVE
MR IMAGING WITH
HISTOPATHOLOGY IN X-LINKED
ADRENOLEUKODYSTROPHY

J. Patrick van der Voorn
Petra J. W. Pouwels
James M. Powers
Wouter Kamphorst
Jean-Jaques Martin
Dirk Troost
Marieke D. Spreeuwenberg
Frederik Barkhof
Marjo S. van der Knaap

Am J Neuroradiol. 2011 Mar; scheduled for publication

ABSTRACT

Background and purpose:

Quantitative MR techniques may improve the pathologic specificity of MR regarding white matter abnormalities. Our purposes were to determine whether ADC, FA, MTR and MRS metabolites correlate with degrees of white matter damage in X-ALD patients; whether differences in ADC, FA and MTR observed in vivo are retained in fresh and formalin-fixed postmortem brain tissue and whether they predict histopathology.

Materials and Methods:

MRS metabolites, MTR, ADC and FA were determined in seven X-ALD patients in three white matter areas (NAWM, active demyelination and complete demyelination) and compared with values obtained in fourteen controls. MTR, ADC and FA were assessed in postmortem brain from fifteen X-ALD patients and five controls. Values were correlated with degree of astrogliosis and density of myelin, axons and cells. Equations to estimate histopathology from MR parameters were calculated by linear regression analysis.

Results:

MRS showed increased mIns, lactate and Cho, and decreased tNAA in living X-ALD patients, values depending on degree of demyelination. MTR, ADC and FA values were different in postmortem than in vivo white matter, but relative differences related to degrees of white matter damage were retained. ADC was high and FA and MTR were low in abnormal white matter. Correlations between histopathologic findings and MR parameters were strong. A combination of ADC and FA predicted pathologic parameters best.

Conclusion:

Changes in quantitative MR parameters, present in living patients and related to severity of white matter pathology, are retained in postmortem brain tissue. MR parameters predict white matter histopathologic parameters.

INTRODUCTION

Conventional MRI has a high sensitivity in the detection of white matter abnormalities. However, it cannot distinguish between different pathologic substrates of white matter lesions. Pathologic findings associated with T2-hyperintensity and T1-hypointensity of the white matter are highly variable and include hypomyelination, demyelination, axonal loss, gliosis, interstitial edema and cystic white matter degeneration (1). Application of additional quantitative MR techniques, such as DTI, MTI and proton MRS, may improve the pathologic specificity of MRI findings and in this way add to the understanding of white matter disease processes. Quantitative MR parameters may also provide reliable measures of the degree of white matter abnormality and be applicable in the monitoring of treatment of white matter disorders.

X-ALD is one of the most common leukodystrophies. In eighty percent of the patients with cerebral involvement, MR imaging shows a large bilateral white matter lesion involving the periventricular and deep white matter of the posterior parietal and occipital lobes (2). Histopathologically, the center of the lesion is characterized by almost complete loss of axons and myelin, accompanied by dense astrogliosis. Active demyelination occurs in the edge of the lesion, accompanied by axonal damage and loss and inflammation (2, 3). Outside the lesion, the white matter is apparently normal. We decided to study the possible contribution of quantitative MR parameters to the prediction of histologic parameters and chose X-ALD as study subject, because this disease allows comparison of large white matter areas with different degrees of myelin loss, axonal loss and gliosis within the same brain slice.

A few studies have investigated the pathologic specificity of quantitative MR parameters in the white matter of postmortem MS brains by comparing them with histopathologic parameters in MS lesions. In a study by Schmierer et al. (4) significant correlations were found between myelin content and MTR and between myelin content and axonal count. In an earlier study by Van Waesberghe et al. (5), T1-signal intensity and MTR were strongly correlated with axonal density. Comparison of MRS and stereotactic brain biopsy findings in MS patients revealed a parallel decrease of tNAA and reduction of axonal density in demyelinating plaques (6). Concomitant increases of Cho and mIns were found to correspond to glial proliferation; elevation of lactate was associated with inflammation (6). A postmortem study correlating diffusion parameters with histopathology in MS patients showed associations between myelin content and FA and ADC (6). A correlative *in vivo* MRI - postmortem histopathology study of the diffusely abnormal white matter in chronic MS showed that decreased FA values were associated with extensive axonal loss and reduced myelin density (8).

In our present study we obtained quantitative MR parameters, including MTR, diffusion parameters and MRS metabolite concentrations, from living patients with the cerebral form of X-ALD and healthy control subjects. We also studied fresh and formalin-fixed postmortem brain slices of X-ALD patients and controls with both MR and histopathology.

The aims of this study were: 1) to determine whether the degree of change in ADC, FA, MTR and MRS metabolites correlates with the degree of white matter damage in vivo and in postmortem brain tissue in X-ALD patients; 2) to determine whether the differences in ADC, FA and MTR observed in vivo are retained in fresh and fixed postmortem brain tissue and, with that, whether application of quantitative MR parameters in studies of postmortem tissue would be justified; and 3) to assess whether ADC, FA and MTR predict histologic changes with regard to amounts of myelin, axons, gliosis and cell density.

MATERIALS AND METHODS

Patients and control subjects

This study was performed with informed consent of patients, control subjects and parents, and with approval of the institutional ethics review board. Table 1 clarifies the numbers of patients and controls included for in vivo and postmortem MR studies and gives age range and median age.

Table 1: Characteristics of patients and control subjects

	In vivo MR study	In vivo MR study	Postmortem MR study	Postmortem MR study
	patients	controls	patients	controls
No. subjects	7	14	15 *,**	5 ***
age range	6-16.7 y	9.3-26.3 y	8.5-52 y	12-68 y
Median age	10 y	17.1 y	15.3 y	24.2 y
No. subjects MTR	5	14	15	5
No. subjects ADC	5	14	15	5
No. subjects FA	5	14	15	5
No. subjects MRS	7	14	n.d.	n.d.

No., number; n.d., not done; * two of these had an MRI 3 and 9 months before death; ** in one of these a brain

MRI was obtained in fresh and formalin-fixed state; *** in all five a brain MRI was obtained in fresh and formalin-fixed state

In a prospective study, we included seven patients with cerebral X-ALD (six with childhood cerebral and one with adolescent cerebral phenotype) and 14 healthy control subjects. These patients received no special treatment apart from hormonal replacement therapy for adrenal insufficiency. Their disease was considered too far advanced for hematopoietic stem cell transplantation. The control subjects were either healthy volunteers or pediatric subjects with normal neurologic examination and normal MR imaging findings. The latter

subjects underwent MRI for reasons like headache and epileptic seizures. In two of the seven X-ALD patients we performed a brain autopsy within 6 hours after death. The interval between their last in vivo MR study and time of death was three and nine months, respectively.

Formalin-fixed brain tissue from the latter two X-ALD patients (both childhood cerebral phenotype), 13 additional X-ALD patients (seven childhood cerebral, six adult cerebral phenotype, cause of death in all patients disease progression), and five non-neurological controls (cause of death cardiac or respiratory failure), was collected from the Neuropathology departments of VU University Medical Center and Academic Medical Center in Amsterdam, University of Antwerp, and the Maryland Brain Bank.

In one of the two X-ALD patients who came to autopsy within six hours after death, as mentioned above, and in five controls a postmortem MR study was performed on unfixed coronal brain slices directly at autopsy. In all 15 X-ALD brains and the five control brains an MR study was performed after at least five weeks of formalin fixation.

MR imaging and spectroscopy

All MR studies of living patients and postmortem specimens were performed on the same 1.5 T MR scanner (Siemens Vision, Erlangen, Germany).

In vivo MR protocol

The in vivo MRI protocol included transverse T2-weighted spin echo images (TR 3000 ms, TE 22, 60 and 120 ms, 1 excitation), and coronal FLAIR images (TR 9000 ms, TE 105 ms, TI 2200 ms, 1 excitation). In five patients axial T1-weighted spin echo images were obtained before and after Gd-DTPA administration.

In all subjects, MRS was performed using a STEAM sequence (TR/TE/mixing time 6000/20/10 ms, 64 accumulations) in a single VOI of 4-6 ml. In control subjects the VOI was placed within parietal white matter. In patients one VOI was selected in the white matter lesion center, one at the lesion edge and one in the NAWM. Metabolite concentrations were calculated using LCModel (9) and expressed as mmol/L. Concentrations were determined for tCr, tNAA, Cho, mIns and Lac (10).

DTI was performed in five patients and in all control subjects with a multi-slice EPI sequence (11) using a reference $b=0$ s/mm² and 8 non-collinear gradient vectors with $b=1044$ s/mm². In transverse orientation, 16 slices of 5 mm were acquired, with a 128 x 128 matrix, using TR 3600 ms and TE 123 ms. The DTI analysis included a correction of eddy current induced distortion, and calculation of eigen values of the diffusion tensor, resulting in maps of ADC and FA (11).

MTI was performed in five patients and in all control subjects with a 3D-FLASH sequence. Two sets of images were obtained, one with (M_s) and one without (M_0) MT saturation pulse (7.68 ms Gaussian RF pulse, 1500 Hz off resonance), using TR 23 ms, TE 4

ms, flip angle 20°, and a 3D slab consisting of 54 transverse slices of 3 mm. MTR maps were created according to $MTR=(1 - M_s/M_0) \times 100\%$.

ROIs corresponding to the MRS VOIs (the x, y and z coordinates of this VOI were noted) were transferred to the equivalent ADC, FA or MTR maps to determine mean values in these ROIs.

Postmortem MR protocol

The postmortem MR study, performed on unfixed coronal brain slices directly at autopsy, was done at room temperature (20-22°C). Five 1cm thick brain slices were placed in a slice holder, which fits in the head coil. The MR pulse sequences as described for living patients were modified and included T2-weighted spin echo images (TR 2000 ms, TE 20 and 45 ms; excitation 1; matrix 160 x 256; field of view 125 x 200 mm, slice thickness 5 mm, in-plane resolution 0.78x0.78 mm) and multi-slab 3D-FLAIR images (turbo spin echo imaging sequence with a turbo factor of 27 (12); six 1cm thick slabs with 8 partitions each, resulting in a slice thickness of 1.25 mm; TR 6500 ms; TE 120 ms; TI 2200 ms; matrix 162 x 256; field of view 127x200 mm, in plane resolution 0.78x0.78 mm). The imaging slices were located at the center of brain slices. To avoid EPI-related distortion artifacts at the interface between air and brain tissue (13, 14), DTI was performed with a diffusion-weighted single shot STEAM sequence (TR 6000ms, TE 65ms, excitations 8; slice thickness 8 mm, field of view 80x128mm; matrix 40x64; flip angle 11°) (12-15), and not with the EPI sequence. Despite lower signal to noise ratio of the STEAM DTI sequence, it yielded similar quantitative results as the EPI DTI sequence in human controls in vivo (data not shown). MRS was not performed in postmortem tissue.

The same MR imaging protocol was followed for imaging of the formalin-fixed brain slices.

Histopathologic analysis

The fixed coronal brain slices were cut in half after imaging, slices were embedded in paraffin, and whole-mount 7µm thick sections were made. Routine staining techniques were applied, including H&E to verify whether histological sections matched corresponding MR images, LFB to determine myelin density, and Bodian silver impregnations to determine axonal density. Immunohistochemical staining with GFAP (DAKO, Copenhagen, Denmark) as the primary antibody was performed to assess the degree of astrogliosis. Only sections containing three different histologic areas were examined: i.e. NAWM, active demyelination (with inflammation) and complete demyelination (without inflammation). In total, 55 areas were examined in 15 patients: 18 areas with complete demyelination, 20 areas with active demyelination and 17 with NAWM. The size of the areas examined was 0.5-1.0cm x 0.5-1.0cm.

H&E-stained sections were used to transfer the examined areas to corresponding ADC, FA and MTR maps by matching the histologic contours with lesion details on the postmortem FLAIR images.

Axonal densities were determined in Bodian-stained sections using a stereological grid (4). Random points of a grid were superimposed on the sections and the number of points crossing axons was measured as a fraction of the total number of points of the grid. Axonal density in areas of active and complete demyelination was expressed as percentage of the axonal density in the NAWM ROI.

Myelin density was quantified by assessing light transmittance on scanned LFB-stained sections using Scion Image for Windows®. The program was set in RGB mode. Within every ROI, the light intensity was assessed in three random areas. Values obtained from each area were averaged and then divided by the light intensity transmitted in the NAWM ROI, to assess relative myelin density.

Numbers of GFAP-positive reactive astrocytes were counted per 40x field in 10 microscopic fields to estimate the degree of astrogliosis. Cell density was determined likewise by counting the total number of nuclei in H&E-stained sections.

Statistical Analysis

Two-sided unpaired t-test was performed to compare in vivo MRS metabolite concentrations and the quantitative parameters MTR, ADC and FA between the white matter lesion center, the lesion edge and the NAWM in patients and white matter in control subjects. Likewise, a two-sided unpaired t-test was performed to compare MTR, ADC and FA values in vivo and in post-mortem brain tissue (fresh and fixed). The significance level was $P < 0.01$.

Analysis of correlations between all parameters in the postmortem samples was performed using SPSS program (SPSS for Windows, version 12.0; SPSS, Chicago, IL). Pearson correlation coefficients to investigate correlations of histopathologic parameters (axonal density, myelin density, cellular density and degree of astrogliosis) with MR parameters (ADC, FA and MTR) in the same ROIs were calculated directly. The variables were normally distributed (Levene's test for normality), or normalized with a log transformation. P-values < 0.01 were considered significant.

Equations to estimate histopathology from MR parameters were calculated by linear regression analysis.

RESULTS

In vivo MR parameters

Illustrations of proton MR spectra, MTR, ADC and FA maps that were obtained in living X-ALD patients are shown in Figure 1. The lesion center showed statistically significant, marked reductions in MTR, FA, and concentrations of tNAA and tCr, and significant increases in ADC and concentrations of mIns and lactate as compared to NAWM. The lesion edge showed similar significant, although less pronounced changes in MTR, ADC, FA, tNAA and mIns; tCr was normal; both Cho and lactated were significantly higher than

in the center of the lesion and in the NAWM. In NAWM of the patients MR parameters were not significantly different from those in cerebral white matter of controls, although all parameters showed a trend for being slightly abnormal. The difference was significant for FA only. Quantified metabolite concentrations and results of DTI and MTI examinations are shown in Table 2.

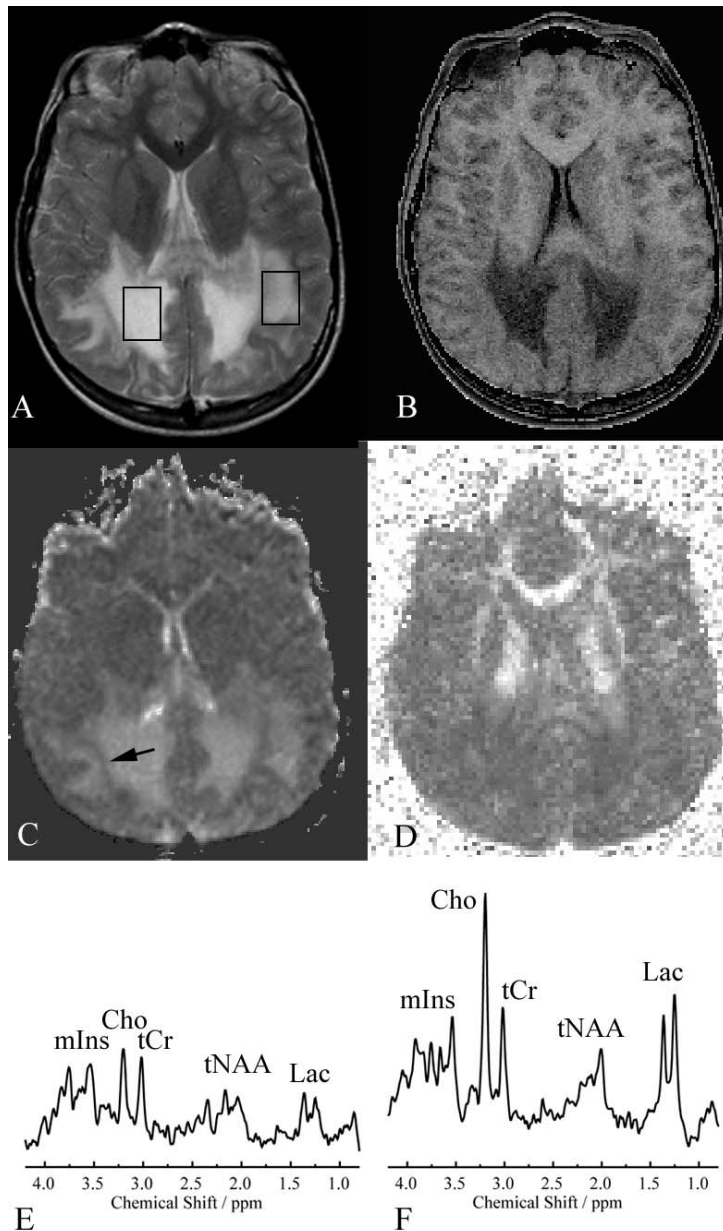


Figure 1
VOI localizations for MRS (STEAM, TR 6000 ms, TE 20 ms, TM 10 ms, 64 accumulations) are shown on a transverse T2-weighted MR image (TR 3000 ms, TE 120 ms, one signal acquired) (a) with MTR (b), ADC (c), and FA (d) maps of the same slice, and corresponding spectra (e and f) in a patient with X-ALD. The VOI placed in the center of the white matter lesion (right hemisphere) showed a very low MTR, high ADC, low FA, very low tNAA, low tCr, high mIns and Cho and high lactate. The VOI at the edge of the lesion showed similar but less pronounced changes, Cho and lactate were higher than in the center of the lesion. Also note the band of low ADC (arrow in c), towards the edge of the lesion.

Table 2: MTR, ADC, FA and MRS metabolite concentrations in cerebral white matter of 7 X-ALD patients and 14 controls (in vivo)

	Center of lesion Mean \pm SD	Edge of lesion Mean \pm SD	NAWM Mean \pm SD	Controls Mean \pm SD
MTR, %	11.5 \pm 3.3*	23.0 \pm 1.5*	29.0 \pm 2.5	31.8 \pm 1.5
ADC, 10 ⁻³ mm ² /s	2.1 \pm 0.4*	1.2 \pm 0.5*	0.83 \pm 0.05	0.81 \pm 0.07
FA	0.20 \pm 0.04*	0.30 \pm 0.05*	0.43 \pm 0.02	0.37 \pm 0.04*
tCr, mmol/L	2.7 \pm 0.9*	4.3 \pm 0.5	4.8 \pm 1.0	4.5 \pm 0.6
tNAA, mmol/L	1.9 \pm 1.8*	4.9 \pm 1.9*	7.2 \pm 0.9	7.7 \pm 1.0
Cho, mmol/L	1.4 \pm 0.9	1.9 \pm 0.3**	1.5 \pm 0.4	1.3 \pm 0.2
mIns, mmol/L	5.0 \pm 1.5*	4.8 \pm 0.6*	4.2 \pm 1.1	3.6 \pm 0.3
Lac, mmol/L	1.8 \pm 2.0*	2.3 \pm 2.5**	0.5 \pm 0.6	0.2 \pm 0.3

* significantly different from NAWM; $p < 0.01$

** significantly different from NAWM and center of lesion; $p < 0.01$

Changes of MTR, ADC and FA values after autopsy and fixation

Five control brains were examined directly after autopsy and after at least five weeks of formalin fixation. Table 3 summarizes the results. A slight reduction in MTR (not reaching the level of significance) as compared to in vivo MTR values was observed after autopsy; a more pronounced, statistically significant reduction was seen after fixation. ADC values were significantly reduced after autopsy as compared to in vivo values and were reduced further after formalin fixation. FA values after formalin fixation were comparable to the FA values in living controls, but they were significantly lower immediately after autopsy.

One X-ALD patient was examined shortly before death, directly after autopsy and after five weeks of formalin fixation. In all stages, the differences in MTR, ADC and FA values between different white matter areas showed a similar trend as the in vivo differences (figure 2 and table 4). In the lesion center, MTR was lower, ADC was higher and FA was lower than in the lesion edge and in NAWM.

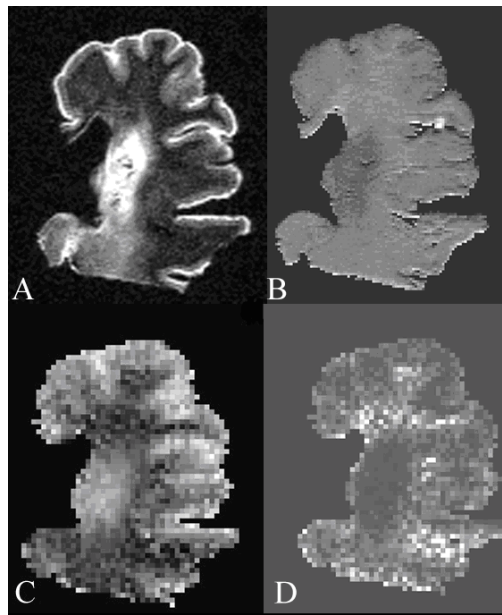


Figure 2
A 3D-FLAIR image (6500/120/2200) (a) and MTR (b), ADC (c), and FA (d) maps at the same position of post mortem X-ALD brain show that differences in MR parameters are retained with postmortem MR tissue, with a low MTR, high ADC and low FA towards the center of the lesion.

Histopathologic parameters

In all 15 X-ALD patients, histopathologic evaluation of the edge of the lesion showed perivascular inflammatory cells with myelin destruction by macrophages and many reactive astrocytes. The lesion center showed a dense mesh of glial fibrils, with scattered astrocytes and almost complete absence of axons, myelin sheaths and oligodendroglia. In the NAWM no evident histologic abnormalities were seen. MR and histopathology of postmortem brain slices are illustrated in figure 3.

Pearson correlations between all MR parameters and histopathologic parameters

The Pearson correlation coefficients (r-values) based on all measurements are given in table 5. The r-values of the correlations differed. Strong correlations were found between the histopathologic and between MR parameters themselves, for instance a strong correlation was found between myelin density and axonal density (0.952). Medium to strong correlations were found between the MR parameters and histopathologic parameters, also illustrated by scatter plots in figure 4 and by the r-values in Table 5.

Table 3: MTR, ADC, and FA values in cerebral white matter of 14 healthy control subjects (in vivo) and in 5 postmortem control brains immediately after autopsy (fresh) and after formalin fixation (fixed)

	In vivo Mean \pm SD	Postmortem, fresh Mean \pm SD	Postmortem, fixed Mean \pm SD
MTR, %	32.0 \pm 1.5	30.6 \pm 0.8	25.0 \pm 0.5*
ADC, 10 ⁻³ mm ² /s	0.80 \pm 0.07	0.25 \pm 0.06*	0.18 \pm 0.05*
FA	0.43 \pm 0.02	0.22 \pm 0.05*	0.37 \pm 0.04

* significantly different from in vivo ; p<0.01

Table 4: MTR, ADC and FA values in cerebral white matter of one X-ALD patient in vivo, immediately after autopsy (fresh) and after formalin fixation (fixed)

	In vivo	Postmortem, fresh	Postmortem, fixed
MTR, %			
Center lesion	9	10	8
Edge lesion	22	18	15
NAWM	29	31	28
ADC, 10 ⁻³ mm ² /s			
Center lesion	2.3	1.40	1.20
Edge lesion	1.2	0.70	0.56
NAWM	0.9	0.50	0.22
FA			
Center lesion	0.22	0.04	0.10
Edge lesion	0.36	0.12	0.22
NAWM	0.50	0.12	0.29

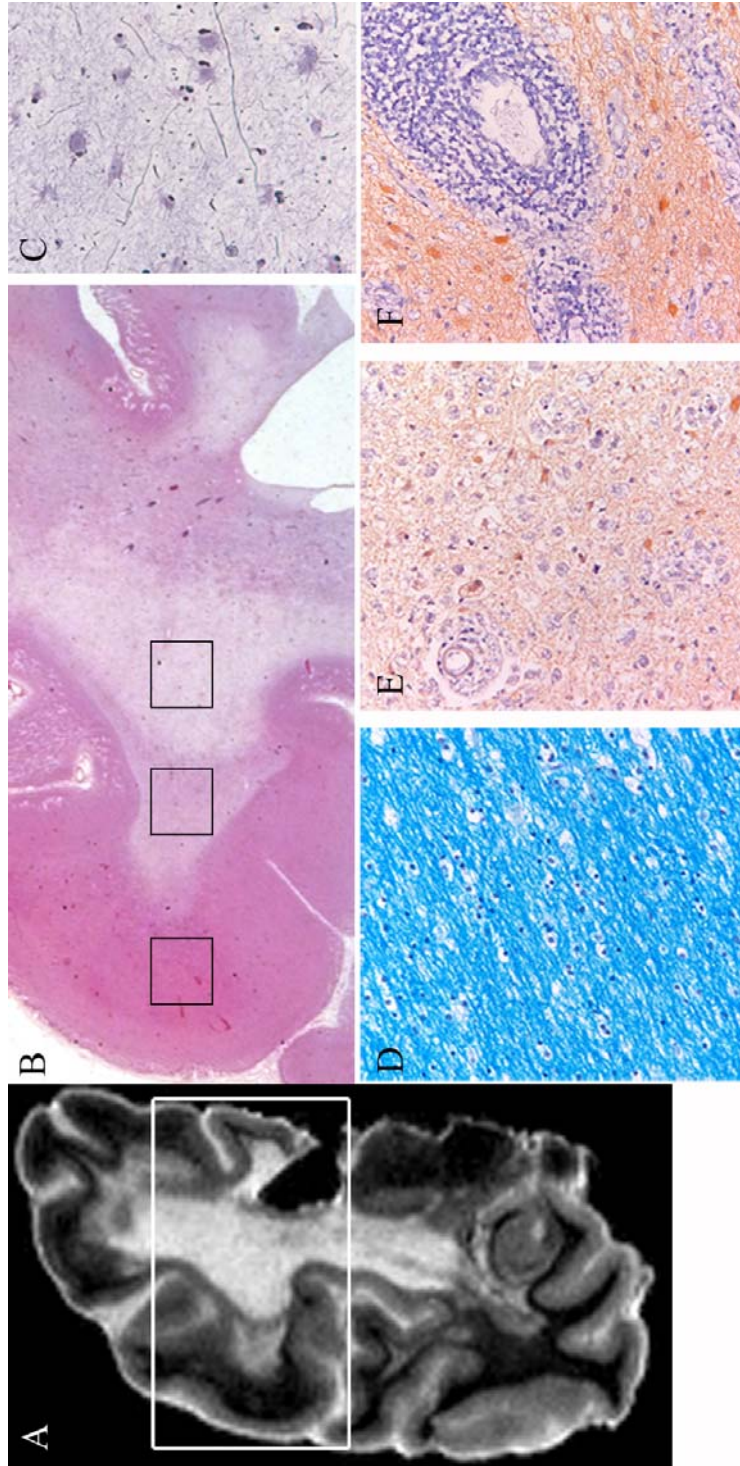


Figure 3 (left)

Correlation of histopathology with MRI in a post mortem X-ALD brain is illustrated. On the whole mount (H&E stained) section (B), which is matched with the corresponding MR image, a 3D-FLAIR image (A), the three different histologic areas are identified and shown in the boxes from left to right: NAWM (D), active demyelination (E-F) and complete demyelination (C). The Luxol fast blue stained section showed dense myelin staining in the NAWM (D). GFAP stained sections (E-F) show intense inflammation with many interstitial macrophages with reactive astrocytes (E) and severe perivascular inflammation (lymphocytes and macrophages) towards the edge with the chronic lesion (F). Bodian-Silver stained section (C) showed very low axonal density in the chronic lesion areas.

Prediction of histopathology by MR parameters

Linear regression analysis showed that FA was the best (positive) predictor with respect to myelin density (myelin density = $-13.7 + 143.9 \times \text{FA}$; R2: 0.587) and that MTR was the best (positive) predictor with respect to cell density (cell density = $5.3 + 4.0 \times \text{MTR}$; R2: 0.440).

Linear regression analysis showed that a combination of ADC (negative predictor for axonal density and positive predictor for astrogliosis) and FA (positive predictor for axonal density and negative predictor for astrogliosis) were the best predictors with respect to axonal density (axonal density = $43.3 + 93.9 \times \text{FA} - 46.2 \times \text{ADC}$; R2: 0.654) and astrogliosis (astrogliosis = $6.3 - 7.2 \times \text{FA} + 9.3 \times \text{ADC}$; R2: 0.568).

In addition, the linear regression analysis showed that ADC and FA combined were sufficient as predictors of all histopathologic parameters (cell density = $35.2 + 63.3 \times \text{FA} - 11.4 \times \text{ADC}$; R2: 0.436; myelin density = $1.9 + 136.1 \times \text{FA} - 16.9 \times \text{ADC}$; R2: 0.592; for prediction of astrogliosis and axonal density see previous paragraph). Adding MTR did not have additional predictive value (i.e. in addition to ADC and FA) with respect to all histopathologic parameters.

DISCUSSION

Effects of death and formalin fixation on MTR, ADC and FA values

Cerebral white matter diffusion parameters and MTR were studied in vivo in normal individuals, in control brains within six hours after death and after at least five weeks of formalin fixation. We also studied one patient with X-ALD in a similar fashion. In unfixed postmortem white matter, MTR values were essentially unchanged, ADC values were greatly reduced and FA was reduced by ~50% as compared to in vivo values. Formalin fixation led to an approximately 20% reduction in MTR and a further decrease in ADC, whereas FA rose to values close to in vivo values.

The differences in MR parameters between in vivo and fresh postmortem white matter are explained by differences in temperature, unavoidable effects of periagonal

problems (especially hypoxia-ischemia) and immediate postmortem decay. In contrast to the in vivo brain temperature of $\sim 37^\circ$ Celsius, postmortem brains are at room temperature ($20\text{-}22^\circ$ Celsius). MTR is practically unaffected by the effects of dying, early postmortem decay (5, 16) and temperature (17). In contrast, diffusivity is significantly affected by the effects of dying and early postmortem decay (18) and also decreases with decreasing temperature (18). In a study of freshly prepared gel-immobilized erythrocyte ghost samples, a temperature decrease from 37° to 20° Celsius was associated with a decrease in ADC of approximately 30% (19). The drop in FA of fresh postmortem tissue has been suggested to reflect a change in membrane permeability due to beginning autolysis of tissue (20). Our findings are in line with these previous studies (5, 16-20).

Formalin fixation has additional effects. Like Schmierer et al. (18), we found that formalin fixation leads to a mild reduction in MTR and causes a mild further reduction of water diffusivity. The FA after fixation is close to the FA in vivo, which implies that directional diffusion is reduced proportionally for all directions, suggesting that tissue architecture is preserved after fixation.

In one X-ALD patient, we studied the MR parameters in areas with different degrees of white matter abnormality in vivo, within six hours after death, and after formalin fixation. We found that the differences in MR parameters were retained in all situations, with a very low MTR, high ADC and low FA in the lesion center and similar but less pronounced changes at the lesion edge. These results indicate that, although the exact values of the MR parameters are influenced by the condition of the brain, they remain applicable and interpretable.

Table 5: Pearson correlations (r-values) for all measurements on formalin-fixed brain tissue of X-ALD patients.

	ADC (*10 ⁻³)	FA	MTR (%)	cells (/40x field)	axonal density (%)	myelin density (%)	astrocytes (/40xfield)
ADC (*10 ⁻³)	1						
FA	-0.772	1					
MTR (%)	-0.728	0.837	1				
cells (/40x field)	-0.560	0.655	0.666	1			
axonal density (%)	-0.740	0.778	0.749	0.728	1		
myelin density (%)	-0.637	0.766	0.727	0.764	0.952	1	
astrocytes (/40xfield)	0.712	-0.707	-0.687	-0.646	-0.830	-0.828	1

All correlations satisfy the criterion of an associated P-value < 0.01 . A negative correlation is indicated with -. All correlation coefficients were above 0.5.

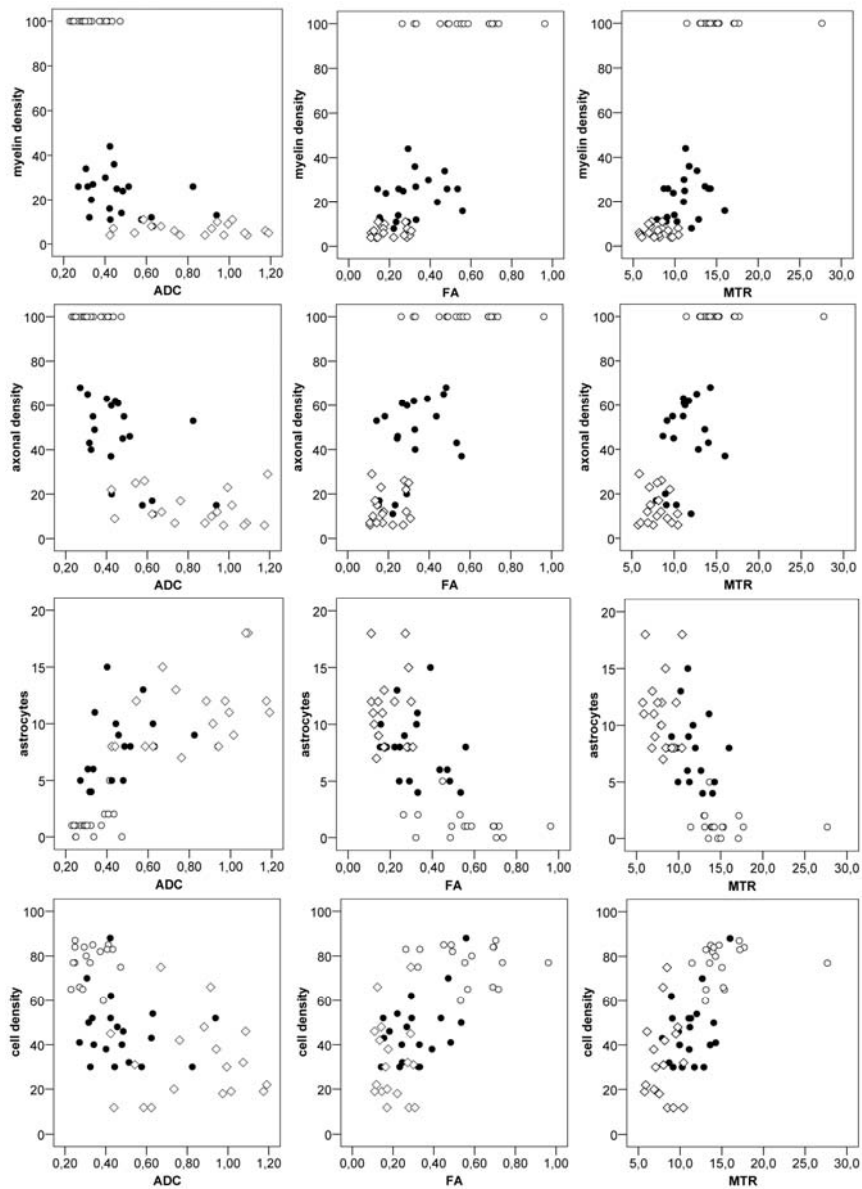


Figure 4
 Relationships between MR parameters [ADC (10-3 mm²/s; first column), FA (second column) and MTR (%; third column)] and histopathologic parameters [myelin density (%; first row), axonal density (%; second row), astrocytes (number/40x field, third row) and cell density (number/40xfield, fourth row)] in post-mortem brain slices are shown. The scatter plots illustrate the correlations between the MR and histopathologic parameters. The corresponding Pearson correlations are given in Table 5.
 ○NAWM, ● active demyelination, ◇ complete demyelination

It should be noted that most studies on the influence of postmortem changes and pathology on MR parameters have been performed on small size samples (cell cultures, rat nervous tissue, small MS lesions, spinal cord) (5, 16-20). Our study used fresh and formalin-fixed human brains and brain slices and focused on large white matter areas. As such the study is an important contribution to the insight into the influence of autolysis, room temperature, formalin fixation and pathology on MR parameters in human brains at 1.5 Tesla. The results of this study are applicable to more routine scanning of postmortem brains, as sometimes performed in clinical situations.

Prediction of histopathology by MR parameters

We performed MRS in a group of living X-ALD patients. Our MRS findings are in agreement with previous reports (21-23). In the center of lesions we found decreased tNAA, low tCr, elevated mIns, and elevated lactate. At the edge of the lesions MRS showed an increase in Cho, some increase in mIns, a more pronounced lactate elevation and less severe decreases in NAA and tCr. The decrease in tNAA can be ascribed to axonal damage and loss, which is more severe in the center than in the edge of the lesion. The increase in Cho is related to enhanced membrane turnover associated with active demyelination and probably also to accumulation of myelin breakdown products, both mainly occurring in the edge of the lesion. The high mIns reflects astrogliosis (24). Elevated lactate is seen in areas of inflammation with infiltrating macrophages, mainly seen in the edge of the lesion. Although in the NAWM of the patients MRS metabolite concentrations were not significantly different from those in the cerebral white matter of controls, there was a trend for being slightly abnormal, with a lower concentration of tNAA and higher concentrations of Cho, tCr, mIns and lactate. Two multi-slice proton MRS imaging studies have reported similar abnormalities in white matter that has a normal appearance on conventional images in X-ALD (25, 26). The finding of a lower tNAA in NAWM indicates slight axonal damage, whereas the increases in concentrations of Cho, tCr, mIns and lactate may represent slightly enhanced myelin turnover and astrocytic reaction, insufficient to lead to signal alterations on conventional MRI.

We did not obtain MRS after death, because spectra are known to change rapidly after death due to postmortem decay (27), obviating the possibility of directly correlating metabolites with histopathologic parameters. However, in the two X-ALD patients in whom we were able to perform an autopsy, histopathology confirmed active demyelination and inflammation in the edge of the lesion, and almost complete loss of axons and myelin with dense gliosis in the inner center of the lesion.

Within the abnormal white matter, both in the edge and the center, both in vivo and postmortem, ADC (a measure for water diffusivity irrespective of direction) was increased, while FA (a measure for the degree of diffusion anisotropy) was decreased, both indicating damage to the tissue matrix. The MTR was decreased, indicating a reduced capacity of the macromolecule-bound protons in brain tissue to exchange magnetization with the

surrounding protons in free water, reflecting damage and loss of myelin sheaths and axonal membranes (28).

We found a progression in abnormality of ADC, FA and MTR from NAWM to lesion periphery to lesion core, indicating primarily a correlation between these parameters and severity of the tissue damage. In contrast, the MRS alterations seen in the lesion edge were different from those seen in the center of the lesion, reflecting the different histopathologic processes. Two earlier MRS studies (1, 29) also stressed the value of spectroscopy regarding pathologic specificity in white matter lesions. In a single-voxel MRS study, combined with DTI and MTI, to investigate whether these techniques could discriminate between different types of white matter pathology, tCr was the best discriminant parameter, followed by Cho, MTR, mIns, ADC, lactate and tNAA (1). A multi-voxel MRSI study demonstrated that metabolite ratios were similar for leukoencephalopathies with a similar pathophysiology and that these ratios may help in the classification of white matter abnormalities (29).

Apart from ADC, FA and MTR being general measures for tissue damage, we searched for more specific correlations between them and histopathologic parameters (myelin density, axonal density, degree of gliosis and cell density). We studied all parameters in the same brain slices. A problem for correlating individual MR parameters with individual histopathologic parameters is that pathologic changes are interdependent. X-ALD is a primarily demyelinating disease, but myelin loss inevitably leads to loss of axons and the resulting tissue damage inevitably leads to astrogliosis. Both inflammation and astrogliosis lead to increased cell density. The strong correlations we observed among the histopathologic parameters themselves, especially myelin density and axonal density, hampered assessment of the specificity of the MR parameters for histopathologic parameters. Despite that, the prediction of histopathologic parameters in the white matter abnormality was reliable using DTI parameters (ADC and FA) only; adding MTR did not improve this prediction significantly. MTR has been used to monitor remyelination in patients with MS, because it is believed to be a specific quantitative marker for myelin density (30, 31). Our results do not support this notion. Most likely, the MTR in these studies reflects the degree of tissue integrity and is only an indirect measure of remyelination.

CONCLUSION

We have demonstrated that differences in quantitative MR parameters, present in living patients and related to severity of white matter pathology, are retained in postmortem brain tissue. We have shown that MR parameters correlate with white matter histopathologic parameters. Quantitative MR parameters can be used to monitor disease progression and the effects of therapy in demyelinating disorders.

ACKNOWLEDGEMENTS

The study was supported by the Dutch Organization for Scientific Research (NWO, Grant 903-42-097) and the Optimix Foundation for Scientific Research. We thank the Brain and Tissue Bank for Developmental Disorders at the University of Maryland, Baltimore, for providing us with formalin-fixed brain tissue of X-ALD patients. We thank Dr. J. Finsterbusch, Hamburg for providing us with the diffusion-weighted single shot STEAM sequence.

REFERENCES

1. Van der Voorn JP, Pouwels PJ, Hart AA et al. Childhood white matter disorders: quantitative MR imaging and spectroscopy. *Radiology* 2006; 241:510-7
2. Van der Knaap MS, Valk J. MR of adrenoleukodystrophy: histopathologic correlations. *Am J Neuroradiol* 1989;10:S12-4
3. Powers JM. Demyelination in peroxisomal diseases. *J Neurol Sci* 2005; 15:206-
4. Schmierer K, Tozer DJ, Scaravilli F, et al. Quantitative magnetization transfer imaging in postmortem multiple sclerosis brain. *J Magn Reson Imaging* 2007; 26:41-51
5. van Waesberghe JH, Kamphorst W, De Groot CJ, et al. Axonal loss in multiple sclerosis lesions: magnetic resonance imaging insights into substrates of disability. *Ann Neurol* 1999; 46:747-54
6. Bitsch A, Bruhn H, Vougioukas V, et al. Inflammatory CNS demyelination: histopathologic correlation with in vivo quantitative proton MR spectroscopy. *Am J Neuroradiol* 1999; 20:1619-27
7. Schmierer K, Wheeler-Kingshott CA, Boulby PA, et al. Diffusion tensor imaging of post mortem multiple sclerosis brain. *NeuroImage* 2007; 35:467-477
8. Seewann A, Vrenken H, van der Valk P, Blezer EL, Knol DL, Castelijns JA, Polman CH, Pouwels PJ, Barkhof F, Geurts JJ. Diffusely abnormal white matter in chronic multiple sclerosis – Imaging and Histopathologic analysis. *Arch Neurol* 2009; 66(5):601-609
9. Provencher SW. Estimation of metabolite concentrations from localized in vivo proton MR spectra. *Magn Reson Med* 1993; 30: 672-679
10. Pouwels PJ, Brockmann K, Kruse B, Wilken B, Wick M, Hanefeld F, Frahm J. Regional age dependence of human brain metabolites from infancy to adulthood as detected by quantitative localized proton MRS. *Pediatr Res* 1999; 46:474-85.
11. Jones DK, Horsfield MA, Simmons A. Optimal strategies for measuring diffusion in anisotropic systems by magnetic resonance imaging. *Magn Reson Med* 1999; 42: 515-525
12. Geurts JJ, Bö L, Pouwels PJ, Castelijns JA, Polman CH, Barkhof F. Cortical lesions in multiple sclerosis: combined postmortem MR imaging and histopathology. *Am J Neuroradiol* 2005; 26(3): 572-577
13. Le Bihan D, Poupon C, Amadon A, Lethimonnier F. Artifacts and pitfalls in diffusion MRI. *J Magn Reson Imaging* 2006; 24:478-488
14. Koch MA, Glauche V, Finsterbusch J, et al. Distortion-free diffusion tensor imaging of cranial nerves and of inferior temporal and orbitofrontal white matter. *Neuroimage* 2002; 17: 497-506
15. Vrenken H, Pouwels PJ, Geurts JJ, et al. Altered diffusion tensor in multiple sclerosis normal-appearing brain tissue: cortical diffusion changes seem related to clinical deterioration. *J Magn Reson Imaging* 2006; 23:628-36
16. Mottershead JP, Schmierer K, Clemence M, et al. High field MRI correlates of myelin content and axonal density in multiple sclerosis--a post-mortem study of the spinal cord. *Neurology* 2003; 250:1293-301

17. Graham SJ, Stanisz GJ, Kecojevic A, et al. Analysis of changes in MR properties of tissues after heat treatment. *Magn Reson Med* 1999; 42:1061-71.
18. Schmierer K, Wheeler-Kingshott CA, Tozer DJ, et al. Quantitative magnetic resonance of postmortem multiple sclerosis brain before and after fixation. *Magn Reson Med* 2008; 59:268-77
19. Thelwall PE, Shepherd TM, Stanisz GJ, Blackband GJ. Effects of temperature and aldehyde fixation on tissue water diffusion properties, studied in an erythrocyte ghost tissue model. *Magn Reson Med* 2006; 56:282-9
20. Shepherd TM, Flint JJ, Thelwall PE, Stanisz GJ, Mareci TH, Yachnis AT, Blackband GJ. Postmortem interval alters the water relaxation and diffusion properties of rat nervous tissue – implications for MRI studies of human autopsy samples. *NeuroImage* 2009; 44: 820-826
21. Van der Knaap MS. Magnetic resonance in childhood white-matter disorders. *Dev Med Child Neurol* 2001; 43: 705-712
22. Pouwels PJ, Kruse B, Korenke GC. Quantitative proton magnetic resonance spectroscopy of childhood adrenoleukodystrophy. *Neuropediatrics* 1998; 29:254-64
23. Confort-Gouny S, Vion-Dury J, Chabrol B, et al. Localised proton magnetic resonance spectroscopy in X-linked adrenoleukodystrophy. *Neuroradiology* 1995; 37:568-575
24. Hattingen E, Raab P, Franz K, et al. Myo-inositol: a marker of reactive astrogliosis in glial tumors? *NMR Biomed* 2008; 21:233-41
25. Eichler FS, Itoh R, Barker PB, et al. Proton MR Spectroscopic and Diffusion tensor brain MR imaging in X-linked adrenoleukodystrophy: initial experience. *Radiology* 2002; 225(1):245-252
26. Eichler FS, Barker PB, Cox C, et al. Proton MR Spectroscopic imaging predicts lesion progression on MRI in X-linked adrenoleukodystrophy: *Neurology* 2002; 58:901-907
27. Ith M, Bigler P, Scheurer E, et al. Observation and identification of metabolites emerging during postmortem decomposition of brain tissue by means of in situ ¹H-magnetic resonance spectroscopy. *Magn Reson Med* 2005; 48(5):915-20
28. Symms M, Jager HR, Schmierer K, Yousry TA. A review of structural magnetic resonance neuroimaging. *J Neurol Neurosurg Psychiatry* 2004; 75(9):1235-44
29. Bizzi A, Castellit G, Bugiani M et al. Classification of childhood white matter disorders using proton MR spectroscopic imaging. *Am J Neuroradiol AJNR* 29:1270-75
30. Schmierer K, Scaravilli F, Altmann DR, et al. Magnetization Transfer Ratio and Myelin in Postmortem Multiple Sclerosis Brain. *Ann Neurol* 2004; 56:407-15
31. Horsfield MA, Barker GJ, Barkhof F, et al. Guidelines for using quantitative magnetization transfer magnetic resonance imaging for monitoring treatment of multiple sclerosis. *J Magn Res Imaging* 2003; 17:389-397